Fatigue Crack Retardation of Low Carbon Steel in Saltwater

K. Tokaji
Associate Professor.

Z. Ando
Professor.

T. Kojima
Graduate Student.

Department of Mechanical Engineering,
Faculty of Engineering,
Gifu University,
1-1 Yanagido, Gifu, Japan

The crack propagation behavior following the application of a single tensile overload in 3 percent saltwater was examined using a low carbon steel, which has a considerably lower static strength than high strength steel used in previous report. Experiments were carried out under sinusoidally varying loads at a load ratio of 0 and a frequency of 10 Hz, and the effects of saltwater were evaluated by comparing with the result in air and result on high strength steel. A single tensile overload was found to cause delayed retardation, just as it did in air. The overload affected zone size was not affected by saltwater and showed the same value in both environments. This observed trend differed from the result on high strength steel in which the overload affected zone size was larger in 3 percent saltwater than in air, and thus it was found that the effect of saltwater on retardation behavior was different even in the similar steels. Retardation cycles were smaller in 3 percent saltwater than in air. Since the overload affected zone size was not affected by saltwater, the decrease in retardation cycles was attributed to the higher rates of fatigue crack propagation in 3 percent saltwater. Thinner specimen showed stronger retardation than thicker one. The behavior at midthickness of thicker specimen showed delayed retardation as well as the result in air. Moreover, the crack propagation behavior following the application of a single tensile overload in 3 percent saltwater was well explained by the crack closure concept.

1 Introduction

Many experimental studies have been performed to investigate fatigue crack retardation behavior following the application of a single tensile overload. However, most of these data have been generated in air (laboratory environment), and thus there currently exists a lack of information in a corrosive environment which is important in practical use.

Chanani [1] examined retardation behavior in 3.5 percent saltwater using three types of aluminum alloy, and found that retardation cycles were smaller in 3.5 percent saltwater than in air. Wei et al. [2] also examined retardation behavior of an aluminum alloy in dehumidified argon, air, and 3.5 percent NaCl solution at room temperature, and found that retardation cycles decreased with increasing aggressiveness of the environment. Moreover, they concluded that since the overload affected zone size was independent of test environment, the decrease in retardation cycles was attributed to the higher rates of a fatigue crack propagation in corrosive environment. On the other hand, the authors [3] examined retardation behavior on a high strength steel in 3 percent saltwater, and found that retardation cycles were invariably larger in 3 percent saltwater than in air. This increase in retardation cycles was attributed to an enlargement of the overload affected zone size in 3 percent saltwater. Although the reason for an enlargement of the overload affected zone size by saltwater is not clear at present time, there exists the definite discrepancy between the result on aluminum alloy and high strength steel. As described at the beginning, since the effects of a corrosive environment on retardation behavior have received very little attention, particularly in steel, it is obscure whether the result by the authors is either a special case for high strength steel used or a common phenomenon for other steels. Using various steels, therefore, further experimental work is needed to confirm phenomenon following the application of a single tensile overload in a corrosive environment. Thereby, it is expected that the reason for the behavior on high strength steel will be apparent.

From the above viewpoints, in this investigation, the fatigue crack propagation behavior following the application of a single tensile overload in 3 percent saltwater was examined using a low carbon steel, which has a considerably lower static strength than high strength steel used in previous report [3]. The effects of saltwater were evaluated by comparing with the result in air [4] and the result on high strength steel [3]. The effect of sheet thickness was also considered.

Contributed by the Materials Division for publication in the JOURNAL OF ENGINEERING MATERIALS AND TECHNOLOGY. Manuscript received by the Materials Division, May 20, 1982.

2 Experimental Procedures

2.1 Material, Specimen and Fatigue Machine. Material used in this study is a 9 mm thick plate of low carbon steel (S10C).

Table 1 Chemical composition of material (%)

C	Si	Mn	P	S	Cu	Ni	Cr
0.13	0.24	0.42	0.011	0.009	0.01	0.01	0.03

Table 2 Mechancial properties of material

Upper yield point	Lower yield point	Tensile strength	Breaking strength on final area	Elongation	Reduction of area
σ_{su} MPa	σ_{sl} MPa	σ_B MPa	σ_T MPa	ϕ %	ψ %
319	254	393	927	36	72

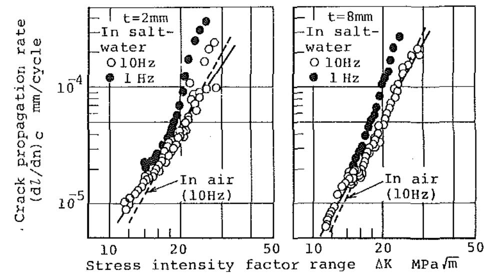

Fig. 1 Relation between crack propagation rate and stress intensity factor range in 3 percent saltwater

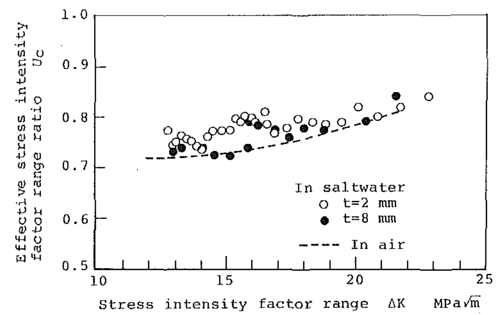

Fig. 2 Relation between effective stress intensity factor range ratio and stress intensity factor range in 3 percent saltwater

Chemical composition and mechanical properties after heat treatment are given in Tables 1 and 2, respectively. The configuration of specimen is the same as that in previous report [3], and the center-cracked specimens with 2 mm and 8 mm thickness were machined so that the axial direction of specimen was parallel to the rolling direction. After machining, the specimen surface was polished by emery-paper in order to facilitate optical observation of fatigue crack and then specimens were heat-treated at 650°C for 1 hr in a vacuum.

Testing was conducted under sinusoidally varying loads at a load ratio of 0 and a frequency of 10 Hz, using a 98 kN capacity, closed loop, servo-controlled testing system. A few specimens were tested at 1 Hz to compare with result at 10 Hz. The fatigue load magnitudes were selected to attain a desired value of stress intensity factor range at a preselected half crack length of 5 mm. Fatigue loading was then interrupted, and a single tensile overload was applied manually. Following the overload, fatigue loading was resumed at the same loading conditions immediately before the overload application. The percent overload {%O.L.} was defined as follows

$$\%\text{O.L.} = \left(\frac{P_{\text{O.L.}} - P_{\max}}{P_{\max}}\right) \times 100$$

where $P_{\text{O.L.}}$ and $P_{\max}$ are overload and maximum cyclic load, respectively. The percent overload used was 30, 40, and 50 percent.

2.2 Test Environment. Test environment is a 3 percent NaCl solution obtained by dissolving NaCl in distilled water. The solution, controlled at 30°C, was contained in a tank, and was circulated at 2.4 liter per hour by a small pump between chambers clamped to the faces of the specimen and the tank.

2.3 Measurement of Crack Length and Crack Opening Load. A traveling microscope with the resolution of 0.01 mm was used to measure crack length. In thicker specimens, an average value of crack lengths measured from both faces of the specimens was used. Periodic cleaning of the specimen surface was performed to avoid the difficulty of measuring crack tip position on an excessively corroded surface.

As shown in previous report [3], a strain gauge was used to measure the crack opening load. Gauges with a gauge length of 1 mm were mounted at various locations on the specimen surface adjacent to the line of the intended crack prolongation. Load versus strain curve was recorded on a $X-Y$ recorder at a frequency of 0.1 Hz. The crack opening load at the location of 1 to 1.5 mm from crack tip was measured.

3 Results and Discussion

3.1 Crack Propagation Behavior Under Constant-Amplitude Loading. The relations between the crack propagation rate $\{(dl/dn)_c\}$ and the stress intensity factor range $\{\Delta K\}$ are shown in Fig. 1. The broken line in the figure represents a regression line of the result obtained previously in air [4]. In both specimens, the crack propagation rates are not affected by the presence of saltwater at the middle and high ΔK range and are slightly enhanced at the low ΔK range. As well as the result in air, the effect of specimen thickness on crack propagation rate is not observed. These results exhibit a "straight line" type of behavior and are represented by a power law of the following form:

$$t = 2\text{ mm} \quad (dl/dn)_c = 5.75 \times 10^{-9}\, \Delta K^{2.99}$$

$$t = 8\text{ mm} \quad (dl/dn)_c = 1.20 \times 10^{-9}\, \Delta K^{3.56}$$

The above equations are indicated by solid line in Fig. 1, and were used to calculate the degree of retardation. The crack propagation rates at 1 Hz, as expected, are faster than those at 10 Hz.

The relation between the effective stress intensity factor range ratio $\{U_c\}$ and ΔK is shown in Fig. 2. The effective stress intensity factor range ratio in 3 percent saltwater is not affected by specimen thickness as well as the result in air indicated by broken line in the figure, and increases with increasing ΔK. Moreover, the effective stress intensity factor range ratio in 3 percent saltwater almost agrees with that in air at the middle and high ΔK range, and is slightly larger than that in air at the low ΔK range.

3.2 Crack Propagation Behavior Following the Application of Single Tensile Overload

3.2.1 The Effect of Saltwater on Crack Propagation Behavior Observed on Specimen Surface. The crack propagation behavior and crack opening behavior observed on specimen surface are shown in Fig. 3. The crack propagation data are reported as the retardation ratio $\{(dl/dn)_d/(dl/dn)_c\}$, which is a ratio of the crack propagation rate for overload test $\{(dl/dn)_d\}$ to that for constant-amplitude loading $\{(dl/dn)_c\}$ versus the crack position $\{d = l - l_{\text{O.L.}}\}$ relative to the point of overload application, and the crack opening data are given by $\{U_d/U_c\}$, which is a ratio of the effective stress intensity factor range ratio for overload test $\{U_d\}$ to that for constant-amplitude loading $\{U_c\}$. The subscript "O.L." denotes the crack length at which an overload was applied. The crack opening behavior will be described later, and the crack propagation behavior is explained here. As can be seen from Fig. 3, the

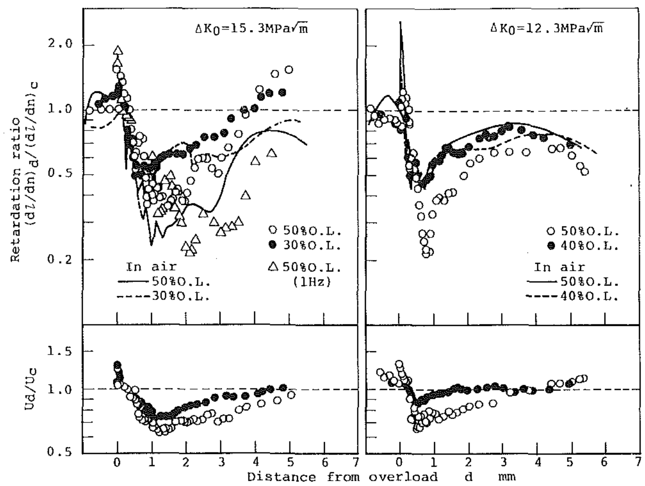

(*a*) $t = 2$ mm

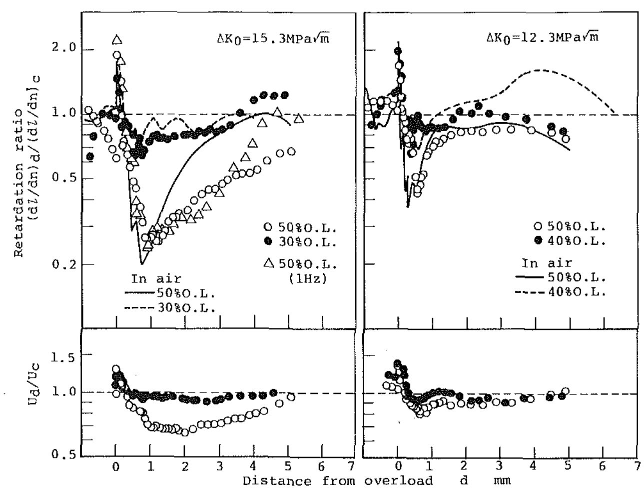

(*b*) $t = 8$ mm

Fig. 3 Crack propagation behavior and crack opening behavior following the application of a single tensile overload in 3 percent saltwater. ΔK_0 represents the base line stress intensity factor range at the point of overload application.

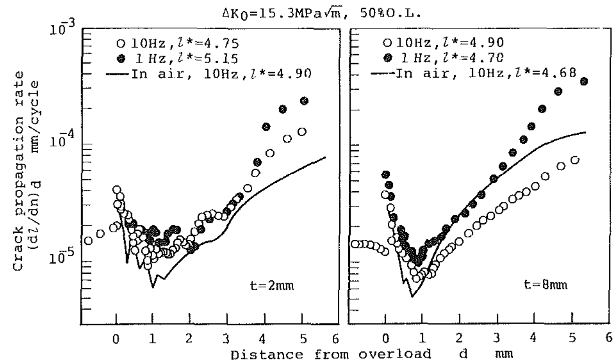

Fig. 4 An example of the arrangement of crack propagation behavior following the application of a single tensile overload by crack propagation rate

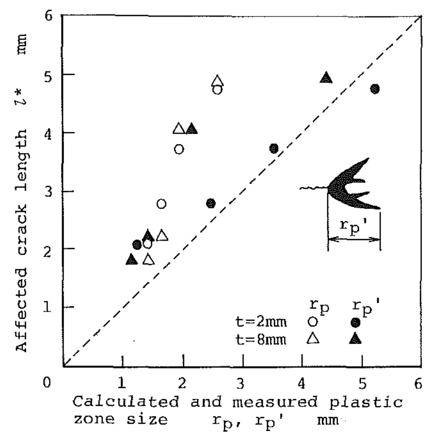

Fig. 5 Relation between overload affected zone size and plastic zone size. r_p and r_p' represent the calculated and measured plastic zone size due to overload application, respectively.

crack propagation behavior shows delayed retardation independent of specimen thickness, base line stress intensity factor range at overload application $\{\Delta K_0\}$ and percent overload, as well as the data in air indicated by solid and broken line [4]. In the result on high strength steel, there was the definite difference between the overload affected zone size $\{l^*\}$ (the distance to return a crack propagation rate commensurate with that for constant-amplitude loading from the point of overload application) in 3 percent saltwater and air, and the overload affected zone size was larger in 3 percent saltwater than in air [3]. In low carbon steel of the present investigation, however, although there exists a slight difference between the behavior through l^* in 3 percent saltwater and air, there is no discernible difference between l^* in both environments. This observed trend is in agreement with result on aluminum alloy by Wei et al. [2]. The result at 1 Hz that the crack propagation rates for constant-amplitude loading were enhanced by the presence of saltwater (see Fig. 1), is shown by open triangle in the figures, and there is no difference between l^* at 1 Hz and 10 Hz.

An example expressed as the crack propagation rate for overload test $\{(dl/dn)_d\}$ versus the crack position relative to the point of overload application is shown in Fig. 4. In thinner specimen, the crack propagation rates through l^* in 3 percent saltwater are higher than those in air, and in thicker specimen, conversely, they are higher in air. The latter result is an only exception in loading conditions tested and in all the other loading conditions the crack propagation rates through l^* were higher in 3 percent saltwater than in air. It is considered that the higher rates are related to the acceleration of crack propagation rates at two ΔK_0 levels for constant-amplitude loading by saltwater (see Fig. 1). Moreover, it is obvious that the crack propagation rates at 1 Hz (closed symbol) are higher than those at 10 Hz (open symbol). This trend also is related to the acceleration of crack propagation rates for constant-amplitude loading.

Figure 5 shows the relation between the overload affected zone size and the plastic zone size due to overload. The calculated plastic zone side $\{r_p\}$ was computed from the following equation for plane stress condition:

$$r_p = \frac{1}{\pi}\left(\frac{K_{\mathrm{O.L.}}}{\sigma_{ys}}\right)^2$$

where σ_{ys} is the yield stress in tension. The measured plastic zone size $\{r_p'\}$ is the practical size at the crack tip caused by the overload application as shown in the figure and was measured by a traveling microscope. The overload affected zone size generally is believed to be related to the overload plastic zone size [5] [6]. In the present investigation, the overload affected zone size corresponds to both the overload plastic zone sizes and appears to be equal to the measured plastic zone size. This observed trend is in agreement with previous result on high strength steel [3].

The relation between the measured plastic zone size and $(K_{\mathrm{O.L.}}/\sigma_{ys})$ is shown in Fig. 6. In the result on high strength steel, the measured plastic zone size was invariably larger in 3

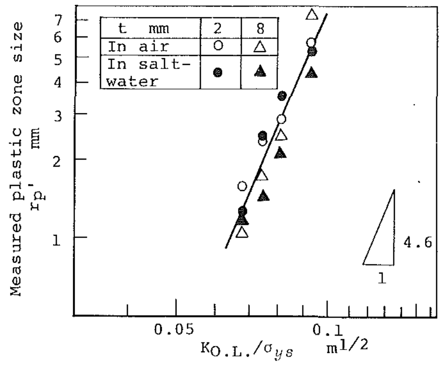

Fig. 6 Log-log plot of measured plastic zone size due to overload application versus $K_{O.L.}/\sigma_{ys}$

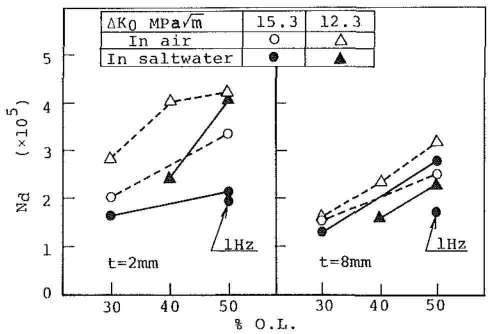

Fig. 7 Relation between retardation cycles and percent overload

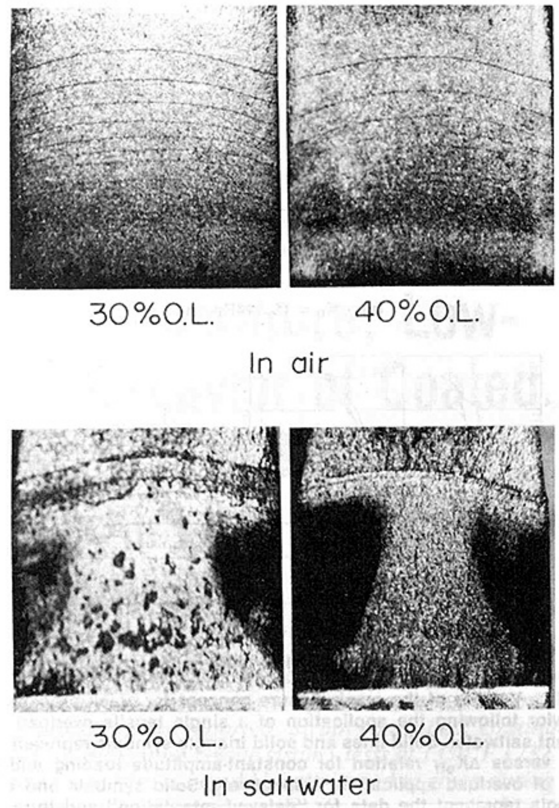

Fig. 8 Crack front geometry for overload test ($\Delta K_0 = 15.3$ MPa$\sqrt{m}$)

percent saltwater than in air at the same value of $(K_{O.L.}/\sigma_{ys})$, and therefore the enlargement of plastic zone size was main reason for stronger retardation in 3 percent saltwater [3]. In low carbon steel, however, the effect of saltwater on the measured plastic zone size is not observed and there is no difference between the measured plastic zone size in 3 percent saltwater and air. Thus, it should be noted that the effect of saltwater on plastic zone size is different between high strength steel and low carbon steel. This observed difference is not due to corrosion dissolution of saltwater, and is probably due to the effect of hydrogen concentrated at a crack tip when considering the difference between static strength of both steels. Further work is needed to confirm this explanation as well as evaluate other possible mechanisms.

The relation between retardation cycles $\{N_d\}$ which are the actual number of cycles required to extend the crack through the overload affected zone and percent overload, is shown in Fig. 7. Retardation cycles are smaller in 3 percent saltwater than in air, excepting only one case ($\Delta K_0 = 15.3$MPa$\sqrt{m}$, 50%O.L. of $t = 8$ mm). Since the overload affected zone size was not affected by 3 percent saltwater, the decrease in retardation cycles may be attributed to higher rates of crack propagation through the overload affected zone in 3 percent saltwater. Retardation cycles at 1 Hz are smaller than those at 10 Hz. Since the overload affected zone size does not alter with frequency, the decrease also may be attributed to higher rates of crack propagation through the overload affected zone (see Fig. 4). Moreover, retardation cycles increase with increasing percent overload and decreasing specimen thickness.

As mentioned above, it was found that the result on low carbon steel shows less retardation in 3 percent saltwater than in air, as well as the results on aluminum alloy by Chanani [1] and Wei et al. [2], and was not in agreement with previous result on high strength steel by the authors [3]. Thus, the effect of saltwater on retardation behavior is different even in both the similar steels and therefore further experimental work using various materials will be needed in this area.

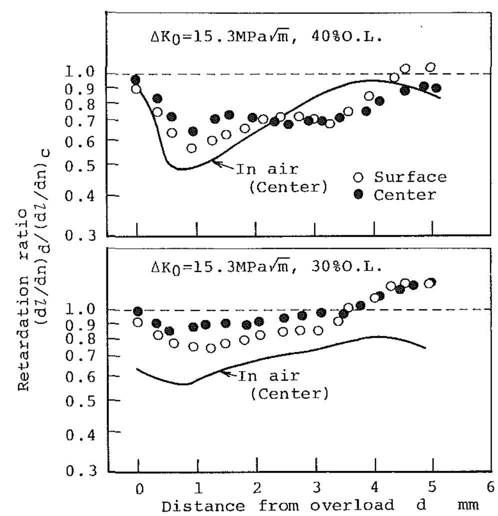

Fig. 9 Comparison of crack propagation behavior following the application of a single tensile overload at midthickness of specimen with that on surface in 3 percent saltwater

3.2.2 Crack Propagation Behavior at Midthickness of Specimen. Figure 8 shows crack front geometry following the application of a single tensile overload. It is found that there is no difference between the crack front geometry in 3 percent saltwater and air.

Figure 9 shows the comparison of the crack propagation behavior at midthickness of specimen with that at surface, obtained beach-mark method. In both loading conditions, the difference between the crack propagation behavior at surface and midthickness is not observed, and both show the delayed retardation. Moreover, as can be seen from the comparison with the behavior at midthickness in air indicated by solid line, it is found that the behavior at midthickness is not af-

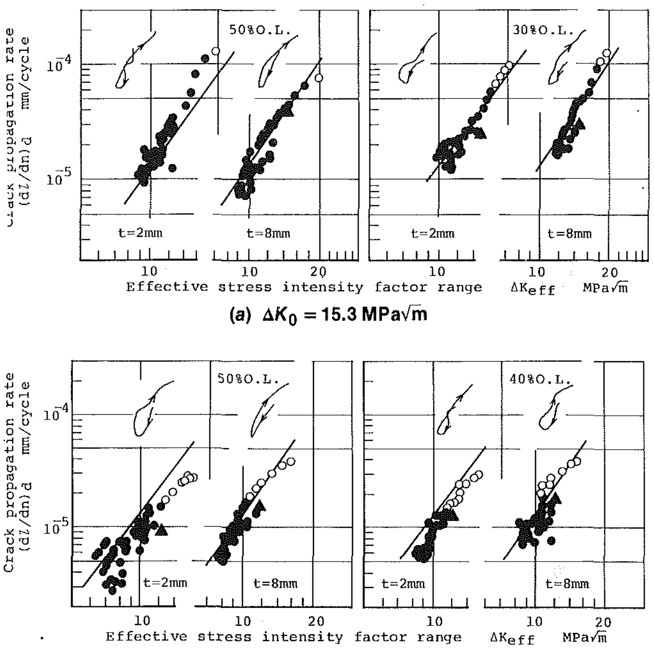

(a) $\Delta K_0 = 15.3$ MPa$\sqrt{m}$

(b) $\Delta K_0 = 12.3$ MPa$\sqrt{m}$

Fig. 10 Validity of the crack closure concept for crack propagation behavior following the application of a single tensile overload in 3 percent saltwater. Solid lines and solid triangle symbols represent the dl/dn versus ΔK_{eff} relation for constant-amplitude loading and the point of overload application, respectively. Solid symbols and open symbols represent the data for "delayed retardation" and those for "recovery," respectively.

fected by the presence of saltwater. It depends on the stress state at crack tip whether the crack propagation behavior following the application of a single tensile overload shows either delayed retardation or retardation (no delay) [4] [7]–[9]. Low carbon steel used has a low static strength (see Table 2), and therefore plane stress state is predominant. Since the stress state is not affected by the presence of saltwater, it can be considered that the behavior at midthickness in both environments shows delayed retardation.

3.2.3 Validity of the Crack Closure Concept for Retardation Behavior. As can be seen from Fig. 3, the crack opening behavior correlates well with delayed retardation behavior of the crack propagation, independent of specimen thickness, ΔK_0 and percent overload. The crack propagation rates for overload test, $(dl/dn)_d$, plotted against ΔK_{eff} instead of ΔK are shown in Fig. 10. Solid lines and curves in the figures give the crack propagation rate versus ΔK_{eff} relation for constant-amplitude loading and the order of the overload test data arranged by ΔK_{eff}, respectively. Thus, the data are arranged to describe a loop according to the order indicated by an arrow from the point of overload application (triangle symbol). As can be seen from the figures, all the experimental points measured in the overload affected zone lie on the crack propagation rate versus ΔK_{eff} relation for constant-amplitude loading independent of specimen thickness, ΔK_0 and percent overload, and thus the crack propagation behavior following the application of a single tensile overload in 3 percent saltwater is well explained by the crack closure concept.

4 Conclusions

The crack propagation behavior following the application of a single tensile overload was examined for a low carbon steel in 3 percent saltwater, and the effects of saltwater were discussed by comparing with the result in air [4] and previous result for high strength steel [3]. The main conclusions of this investigation are as follows:

(1) A single tensile overload caused delayed retardation, just as it did in air. The overload affected zone size was not affected by saltwater and showed the same value in both environments. This observed trend differed from the result on high strength steel in which the overload affected zone size was larger than in 3 percent saltwater than in air, and thus it was found that the effect of saltwater on retardation behavior was different even in the similar steels. This suggests the necessity of further experimental study using various materials.

(2) Retardation cycles were smaller in 3 percent saltwater than in air. Since the overload affected zone size was not affected by saltwater, this decrease in retardation cycles may be attributed to the higher rates of fatigue crack propagation in 3 percent saltwater.

(3) The thinner specimen showed the stronger retardation than the thicker one.

(4) The practical plastic zone size (measured plastic zone size) due to overload application was not affected by saltwater, and showed the same value in both environments. This trend also differed from the result on high strength steel in which the measured plastic zone size was invariably larger in 3 percent saltwater than in air.

(5) The crack propagation behavior at midthickness of specimen following the application of a single tensile overload showed delayed retardation as well as the result in air.

(6) The crack propagation behavior following the application of a single tensile overload in 3 percent saltwater was well explained by the crack closure concept.

Acknowledgment

The authors express their sincere appreciation to Messrs. K. Katagiri and N. Kunishima for their assistance with the experimental work.

References

1 Chanani, G. R., ASTM STP 642, 1978, p. 51.

2 Wei, R. P., Fenelli, N. E., Unangst, K. D., and Shih, T. T., ASME Journal of Engineering Materials and Technology, Vol. 102, 1980, p. 280.

3 Tokaji, K., Ando, Z., Imai, T., and Kojima, T., ASME Journal of Engineering Materials and Technology, Vol. 105, 1983, p. 88.

4 Tokaji, K., Ando, Z., Imai, T., and Morikawa, K., *J. Soc. Mat. Sci. Japan*, Vol. 31, 1982, p. 51.

5 Von Euw, E. F. J., Hertzberg, R. W., and Roberts, R., ASTM STP 513, 1972, p. 230.

6 Mills, W. J., and Hertzberg, R. W., *Engng. Fract. Mech.*, Vol. 7, 1975, p. 705.

7 Bernard, P. J., Lindley, T. C., and Richards, C. E., *Metal Science*, Vol. 11, 1977, p. 390.

8 Tokaji, K., Ando, Z., Imai, T., and Morikawa, K., *Proceedings of the 24th Japan Cong. Mat. Research*, 1981, p. 105.

9 Kikukawa, M., Jono, M., Kanaya, T., and Sugata, J., *Proc. JSME Autumn Meeting*, No. 810-11, 1981, p. 143.